

Intelligent Decision Support System for Planetary Defense under Mixed Aleatory/Epistemic Uncertainties

1st Yirui Wang

*Aerospace Centre of Excellence, University of Strathclyde
National Space Science Center, Chinese Academy of Sciences
yirui.wang@strath.ac.uk*

2nd Massimiliano Vasile

*Aerospace Centre of Excellence, University of Strathclyde
massimiliano.vasile@strath.ac.uk*

Abstract—This paper studies the application of Machine Learning techniques in Planetary Defense. To quickly respond to an asteroid impact scenario, an Intelligent Decision Support System is proposed to automatically decide if a deflection mission is necessary, and then select the most effective deflection strategy. This system consists of two sub-systems: the first one is named as Asteroid Impact Scenarios Identifier, and the second one is named as Asteroid Deflection Strategies Selector. The input to the Asteroid Impact Scenarios Identifier is the warning time, the orbital parameters and the diameter of the asteroid and the corresponding uncertainties. According to the Probability of Collision and the corresponding confidence, the output is the decision of action: the deflection is needed, no deflection is needed, or more measurements need to be obtained before making any decision. If the deflection is needed, the Asteroid Deflection Strategies Selector is activated to output the most efficient deflection strategy that offers the highest probability of success. The training dataset is produced by generating thousands of virtual impact scenarios, sampled from the real distribution of Near-Earth Objects. A robust optimization is performed, under mixed aleatory/epistemic uncertainties, with five different deflection strategies (Nuclear Explosion Device, Kinetic Impactor, Laser Ablation, Gravity Tractor and Ion Beam Shepherd). The robust performance indices are considered as the deflection effectiveness, which is quantified by the change of impact probability pre and post deflection. We demonstrate the capabilities of Random Forest, Deep Neural Networks and Convolutional Neural Networks at classifying impact scenarios and deflection strategies. Simulation results suggest that the proposed system can quickly provide decisions to respond to an asteroid impact scenario. Once trained, the Intelligent Decision Support System, does not require re-running expensive simulations and is, therefore, suitable for the rapid prescreening deflection options.

Index Terms—Robust Optimisation, Machine Learning, Asteroid Deflection, Epistemic Uncertainty

I. INTRODUCTION

Asteroid impact poses a major threaten to all life on the Earth. Several serious impact events through history, from the Chixulub Event 66 million years ago, to the Tunguska Event in 1908 down to the Chelyabinsk Event in 2013, have concretely demonstrated the risk of an impact with asteroids and comets. Most recently, on July 25, 2019, the asteroid 2019 OK (about

80-m in diameter) passed by the Earth from a distance of 73,000 km just a few hours after its discovery. Planetary defense is the term used to encompass all the capabilities needed to detect the possibility and warn of potential asteroid or comet impacts with Earth, and then either prevent them or mitigate their possible effects [1].

In the planning and decision making process that precedes the implementation of an asteroid deflection missions, such as identifying hazardous asteroids and selecting asteroid deflection strategies, there is a considerable amount of uncertainty affecting any decision [2, 3]. In addition to the aleatory uncertainties which derive from the inherent randomness that are irreducible, the epistemic uncertainties that are caused by the lack of knowledge and limited experimental opportunities cannot be ignored. For example, the uncertainty interval of asteroid Itokawa's mass before and after Hayabusa 1 mission, narrowed from $[2.7 \times 10^{10}, 6.5 \times 10^{10}]kg$ to $[3.40 \times 10^{10}, 3.76 \times 10^{10}]kg$ [4, 5]. Both aleatory and epistemic uncertainties should be considered during the decision making process. Although Dempster-Shafer theory of evidence (DSt) [6] can deal with both types of uncertainties in its framework, incorporating epistemic uncertainty into the robust optimisation framework will be computationally expensive [7]. Machine Learning (ML) offers a potentially interesting solution to reduce this cost, therefore, deliver a rapid decision support on identifying hazardous asteroids and selecting effective deflection strategies under mixed aleatory and epistemic uncertainties.

This paper proposes an Intelligent Decision Support System (IDSS) that consists of two sub-systems: Asteroid Impact Scenarios Identifier and Asteroid Deflections Strategies Selector. The diagram of IDSS is shown in Figure 1. The input to the Asteroid Impact Scenarios Identifier is the warning time, the orbital parameters and the diameter of the asteroid and the corresponding uncertainties. The output is the action decision: the deflection is needed, no deflection is needed, or more measurements need to be obtained before making any decision. If the deflection is needed, the Asteroid Deflection Strategies Selector is activated to output the most efficient deflection strategy that offers the highest probability of success. Five as-

teroid deflection strategies are considered: Nuclear Explosions Device (NED) [8], Kinetic Impactor (KI) [9], Laser ablation (LA) [10], Gravitational Tractor (GT) [11] and Ion Beam Shepherd (IBS) [12]. IDSS is based on a machine learning algorithm that is trained on the dataset of virtual impactors and deflections scenarios. Three different Machine Learning techniques are compared in this paper: Random Forest (RF), Deep Neural Networks (DNNs) and Convolutional Neural Networks (CNNs).

II. METHODOLOGY

This section will briefly introduce our proposed approach to uncertainty quantification and propagation, the model of probability of collision, deflection dynamics, as well as the method of Evidence-based robust optimisation.

A. Uncertainty quantification and propagation

1) *Uncertainty quantification*: In this paper, the mixed aleatory and epistemic uncertainties are defined as the distribution type is deterministic (Gaussian distribution is considered), but the intervals of distribution parameters are non deterministic. The real values of orbital elements $\tilde{\mathbf{x}}$ and absolute visual magnitude \tilde{H} under uncertainties can be described as

$$\tilde{\mathbf{x}} \approx \mathbf{x} + \Delta \mathbf{x} \quad (1)$$

$$\tilde{H} \approx H + \Delta H \quad (2)$$

while \mathbf{x} and H are nominal values, and $\Delta \mathbf{x}$ and ΔH are corresponding uncertainty values. Absolute visual magnitude H [13] is used for estimating the mass of the asteroid

$$\begin{cases} D = \frac{1329}{10^{0.2H} \sqrt{p}} \\ m_{\text{Ast}} = \frac{1}{6} \pi D^3 \rho \end{cases} \quad (3)$$

where assumes the asteroid's density ρ is 2.6 g/cm^3 , albedo p is 0.154.

Let $\lambda_{\mathbf{x}}$ and λ_H be the distribution parameters (mean value μ and standard deviation σ) of $\Delta \mathbf{x}$ and ΔH . Then, $\tilde{\mathbf{x}}$ and \tilde{H} under mixed aleatory and epistemic uncertainties can be modelled as

$$\begin{aligned} \tilde{\mathbf{x}} &\approx \mathbf{x} + \Delta \mathbf{x}(\lambda_{\mathbf{x}}), & \lambda_{\mathbf{x}} &= [\mu_{\mathbf{x}}^T, \sigma_{\mathbf{x}}^T] \\ \tilde{H} &\approx H + \Delta H(\lambda_H), & \lambda_H &= [\mu_H^T, \sigma_H^T] \end{aligned} \quad (4)$$

while $\lambda_{\mathbf{x}}$ and λ_M are subject to the condition of $\{\lambda_{\mathbf{x}} | \underline{\lambda}_{\mathbf{x}} \leq \lambda_{\mathbf{x}} \leq \bar{\lambda}_{\mathbf{x}}\}$ and $\{\lambda_H | \underline{\lambda}_H \leq \lambda_H \leq \bar{\lambda}_H\}$. For the current version of IDSS, we only consider the intervals of standard deviation σ instead of mean value μ , that is, $\lambda_{\mathbf{x}} = \sigma_{\mathbf{x}}^T$ and $\lambda_H = \sigma_H^T$. The covariance matrix of orbital elements $\Sigma_{\mathbf{x}}$ at the initial state is defined as

$$\Sigma_{\mathbf{x}} = \mathbf{A} \mathbf{A}^T, \quad \mathbf{A} = \text{diag}(\sigma_a, \sigma_e, \sigma_i, \sigma_\Omega, \sigma_\omega, \sigma_M) \quad (5)$$

When the epistemic uncertainties are introduced through Dempster-Shafer theory of evidence (DSt), the uncertain quantities are modelled with intervals with associated Basic Probability Assignment (*bpa*). Consider for each component u_i of the uncertainty vector \mathbf{u} , a collection of s_i intervals:

$$I_i = \{e_{ij} | u_i \in e_{ij}, j = 1, \dots, s_i\} \quad (6)$$

with a $bpa(e_{ij}) \in [0, 1]$ associated to each interval. Then the uncertainty set U is given by the Cartesian product $U = I_1 \times I_2 \times \dots \times I_n$ and we can define a focal element $\gamma_q = e_{1J_q(1)} \times e_{2J_q(2)} \times \dots \times e_{iJ_q(i)} \times \dots \times e_{nJ_q(n)}$ with associated $bpa(\gamma_q) = \prod_i bpa_{e_{iJ_q(i)}}$ where the vector \mathbf{J}_q has n components and contains a permutation of indexes j . We can now define the set A_ν as:

$$A_\nu = \{f(\mathbf{d}, \mathbf{u}) | f(\mathbf{d}, \mathbf{u}) < \nu, \mathbf{d} \in D, \mathbf{u} \in U\} \quad (7)$$

the cumulative Belief (*Bel*) and Plausibility (*Pl*) associated to proposition in Eq.(7) can be used to estimate the confidence:

$$Bel(A_\nu) = \sum_{\gamma_q \subseteq A_\nu} bpa(\gamma_q) \quad (8)$$

$$Pl(A_\nu) = \sum_{\gamma_q \cap A_\nu \neq \emptyset} bpa(\gamma_q) \quad (9)$$

2) *Uncertainty propagation*: The Unscented Transformation (UT) [14] is used for uncertainty propagation in this paper. UT technique was proposed to calculate the mean value and the covariance matrix of probability distribution of a random variable that undergoes a nonlinear transformation [15]. The basic idea is that, instead of performing a higher order analysis, the probability distribution at a future time can be approximated by using a set of representative points, called sigma points.

Given the n -dimensional random variable \mathbf{x} with a mean value $\bar{\mathbf{x}}$ and a covariance \mathbf{P}_{xx} , and a nonlinear transformation $\mathbf{y} = \mathbf{f}(\mathbf{x})$, the UT is used to estimate the mean value $\bar{\mathbf{y}}$ and the covariance \mathbf{P}_{yy} of the random variable \mathbf{y} by the following steps.

① Calculate the sigma points \mathcal{X} and their weights $W_m^{(i)}, W_c^{(i)} (i = 0, 1, \dots, 2n)$:

$$\begin{aligned} \mathcal{X}^{(0)} &= \bar{\mathbf{x}}, & W_m^{(0)} &= \frac{\lambda}{(n + \lambda)}, & W_c^{(0)} &= W_m^{(0)} + (1 - \alpha^2 + \beta) \\ \mathcal{X}^{(j)} &= \bar{\mathbf{x}} + \left(\sqrt{(n + \lambda) \mathbf{P}_{xx}} \right)_j, & W_m^{(j)} &= \frac{1}{2(n + \lambda)}, \\ & & W_c^{(j)} &= W_m^{(j)} \\ \mathcal{X}^{(n+j)} &= \bar{\mathbf{x}} - \left(\sqrt{(n + \lambda) \mathbf{P}_{xx}} \right)_j, & W_m^{(n+j)} &= \frac{1}{2(n + \lambda)}, \\ & & W_c^{(n+j)} &= W_m^{(n+j)} \end{aligned} \quad (10)$$

where $j = 1, 2, \dots, n; n \in \mathbb{N}$ is the dimension of the state vector; β should be 2 for Gaussian distributions; and $(\dots)_j$ means the j^{th} column vector of the matrix.

② Obtain the set of the transformed sigma points $\mathcal{Y}^{(i)}$:

$$\mathcal{Y}^{(i)} = \mathbf{f}(\mathcal{X}^{(i)}) \quad (11)$$

③ The mean value and the covariance are calculated by using the weights and transformed sigma points as follows:

$$\bar{\mathbf{y}} = \sum_{i=0}^{2n} W_c^{(i)} \mathcal{Y}^{(i)} \quad (12)$$

$$\mathbf{P}_{yy} = \sum_{i=0}^{2n} W_c^{(i)} \left[\mathcal{Y}^{(i)} - \bar{\mathbf{y}} \right] \left[\mathcal{Y}^{(i)} - \bar{\mathbf{y}} \right]^T \quad (13)$$

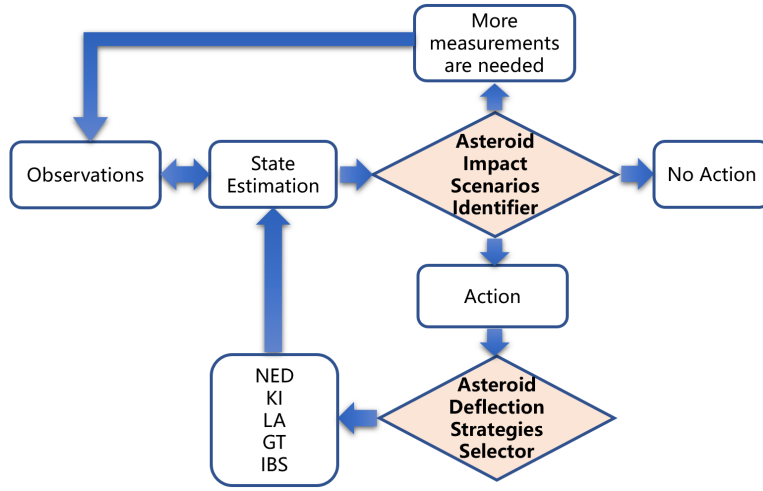


Figure 1. Diagram of Intelligent Decision Support System for Planetary Defense.

B. Asteroid Probability of Collision

The B-plane reference frame $\langle \hat{\xi}, \hat{\eta}, \hat{\zeta} \rangle$, which is centred at the Earth's mass point at the expected impact epoch (time of Minimum Orbit Intersection Distance, MOID), is introduced to quantify the asteroid Probability of Collision (P_c). The asteroid's position on the B-plane at the time of MOID is $\tilde{\mathbf{x}}_{\xi\zeta} = (\xi, \zeta)$. Defining the covariance matrix $(\boldsymbol{\mu}_{\xi\zeta}, \boldsymbol{\Sigma}_{\xi\zeta}) = \boldsymbol{\Phi}(\boldsymbol{\mu}_{\mathbb{a}}, \boldsymbol{\Sigma}_{\mathbb{a}})$, where $\boldsymbol{\Phi}$ is the nonlinear function which maps the covariance matrix of the asteroid from Keplerian elements to (ξ, ζ) on the B-plane. Then, P_c is computed by integrating the uncertainty ellipsoid, centered on the asteroid's mass point and projected on the B-plane, over the closed region $\mathcal{B}((0, 0), R)$ defined by Earth's radius (assuming $R_E = 6378km$ in this paper).

$$P_c(\mathbf{x}_{\xi\zeta}; \boldsymbol{\mu}_{\xi\zeta}, \boldsymbol{\Sigma}_{\xi\zeta}) = \frac{1}{2\pi\sqrt{|\boldsymbol{\Sigma}_{\xi\zeta}|}} \iint_{\mathcal{B}((0,0),R)} \mathbf{pdf} \, d\xi \, d\zeta \quad (14)$$

where $\mathbf{pdf} = e^{-\frac{1}{2}[(\mathbf{x}_{\xi\zeta} - \boldsymbol{\mu}_{\xi\zeta})^T \boldsymbol{\Sigma}_{\xi\zeta}^{-1} (\mathbf{x}_{\xi\zeta} - \boldsymbol{\mu}_{\xi\zeta})]}$. Paterna's method [16] is used for calculating P_c due to the fact that computational efficiency is advantageous when large numbers of P_c evaluations are performed.

C. Deflection Dynamics

According to the different deflection mechanism, deflection strategies can be divided into two categories: Impulsive methods (NED, KI) and Slow-push methods (LA, GT, IBS). This section briefly recalls the deflection dynamics formulas to calculate the P_c , where the momentum transfer models of different strategies refer to Ref. [12]

1) *Impulsive methods*: The effect of an impulsive change in the velocity of the asteroid induces a variation of its orbit and related orbital elements. According to Ref. [9], the deflection position on the impact plane can be calculated analytically by rewriting $\delta\mathbf{v}$ in a tangential, normal, out-of-plane reference frame

$$\delta\mathbf{v} = [\delta v_t, \delta v_n, \delta v_h]^T \quad (15)$$

The variation of Keplerian elements at the time of deflection (caused by $\delta\mathbf{v}$ and ephemeris uncertainties) can be calculated by

$$\begin{aligned} \delta a &= \frac{2\tilde{a}^2\tilde{v}}{\mu} \delta v_t \\ \delta e &= \frac{1}{\tilde{v}} \left[2(\tilde{e} + \cos\tilde{\theta}_d) \delta v_t - \frac{\tilde{r}}{\tilde{a}} \sin\tilde{\theta}_d \delta v_n \right] \\ \delta i &= \frac{\tilde{r} \cos\tilde{\theta}_d^*}{\tilde{h}} \delta v_n \\ \delta \Omega &= \frac{\tilde{r} \sin\tilde{\theta}_d^*}{\tilde{h} \sin\tilde{i}} \delta v_h \\ \delta \omega &= \frac{1}{\tilde{e}\tilde{v}} \left[2\sin\tilde{\theta}_d \delta v_t + (2e + \frac{\tilde{r}}{\tilde{a}} \cos\tilde{\theta}_d) \delta v_n \right] - \\ &\quad \frac{\tilde{r} \sin\tilde{\theta}_d^* \cos\tilde{i}}{\tilde{h} \sin\tilde{i}} \delta v_h \\ \delta M_d &= -\frac{\tilde{b}}{\tilde{e}\tilde{a}\tilde{v}} \left[2 \left(1 + \frac{\tilde{e}^2\tilde{r}}{\tilde{p}} \right) \sin\tilde{\theta}_d \delta v_t + \frac{\tilde{r}}{\tilde{a}} \cos\tilde{\theta}_d \delta v_n \right] \end{aligned} \quad (16)$$

due to the change of semi-major axis, the change in the mean anomaly at the time of MOID is given by

$$\delta M_n = \delta n \Delta t = \left(\sqrt{\frac{\mu}{a^3}} - \sqrt{\frac{\mu}{(a + \delta a)^3}} \right) (t_{\text{MOID}} - t_d) \quad (17)$$

therefore, the total variation in the mean anomaly δM between the unperturbed and the deflected orbit is $\delta M = \delta M_d + \delta M_n$.

The position of the deflected asteroid with respect to the undeflected one at the true anomaly θ_{MOID} along the orbit of

the undeflected asteroid is [17]:

$$\begin{aligned}
 \delta x_r &\approx \frac{r}{a} \delta a + \frac{ae \sin \theta_{\text{MOID}}}{\sqrt{1-e^2}} \delta M - a \cos \theta_{\text{MOID}} \delta e \\
 \delta y_\theta &\approx \frac{r}{(1-e^2)^{3/2}} (1 + e \cos \theta_{\text{MOID}})^2 \delta M + r \delta \omega + \\
 &\quad \frac{r \sin \theta_{\text{MOID}}}{(1-e)} (2 + e \cos \theta_{\text{MOID}}) \delta e + r \cos i \delta \Omega \\
 \delta z_h &\approx r (\sin \theta_{\text{MOID}}^* \delta i - \cos \theta_{\text{MOID}}^* \sin i \delta \Omega)
 \end{aligned} \tag{18}$$

where $\delta \mathbf{r} = [\delta x_r, \delta y_\theta, \delta z_h]^T$ is the displacement vector in a radial, transversal, out-of-plane reference frame attached to the undeflected asteroid. The deflection vector $\tilde{\mathbf{x}}_b$ in the B-plane coordinates can be expressed as

$$\tilde{\mathbf{x}}_b(t_{\text{MOID}}) = \begin{bmatrix} \hat{\xi} & \hat{\eta} & \hat{\zeta} \end{bmatrix}^T \begin{bmatrix} \hat{r} & \hat{\theta} & \hat{h} \end{bmatrix} \delta \mathbf{r} \quad (\delta \mathbf{v}; \Delta \mathbf{a}) \tag{19}$$

where

$$\hat{\eta} = \frac{\mathbf{U}(t_{\text{MOID}})}{\|\mathbf{U}(t_{\text{MOID}})\|}, \quad \hat{\xi} = \frac{\mathbf{v}_E(t_{\text{MOID}}) \times \hat{\xi}}{\|\mathbf{v}_E(t_{\text{MOID}}) \times \hat{\xi}\|}, \quad \hat{\zeta} = \frac{\hat{\xi} \times \hat{\eta}}{\|\hat{\xi} \times \hat{\eta}\|} \tag{20}$$

$$\begin{aligned}
 \hat{r} &= \frac{\mathbf{r}_{\text{Ast}}(t_{\text{MOID}})}{\|\mathbf{r}_{\text{Ast}}(t_{\text{MOID}})\|}, \quad \hat{h} = \frac{\mathbf{r}_{\text{Ast}}(t_{\text{MOID}}) \times \mathbf{v}_{\text{Ast}}(t_{\text{MOID}})}{\|\mathbf{r}_{\text{Ast}}(t_{\text{MOID}}) \times \mathbf{v}_{\text{Ast}}(t_{\text{MOID}})\|}, \\
 \hat{\theta} &= \frac{\hat{h} \times \hat{r}}{\|\hat{h} \times \hat{r}\|}
 \end{aligned} \tag{21}$$

2) *Slow-push methods*: In the general case of slow-push strategies, the variation of the orbital parameters is calculated by integration of equinoctial form of Gauss equations from the time t_d when the deflection action starts until the time t_e when the deflection action stops, which is performed by a Runge-Kutta-Fehlberg 7(8) numerical method. The position of the deflected asteroid with respect to the undeflected one at the true anomaly θ_{MOID} along the orbit of the undeflected asteroid is calculated by (18)-(21).

$$\begin{aligned}
 \frac{da}{dt} &= \frac{2}{B} \sqrt{\frac{\tilde{a}^3}{\mu}} \left[(\tilde{P}_2 \sin \tilde{L} - \tilde{P}_1 \cos \tilde{L}) a_r + \Phi(\tilde{L}) a_\theta \right] \\
 \frac{dP_1}{dt} &= B \sqrt{\frac{\tilde{a}}{\mu}} \left[-a_r \cos \tilde{L} + \left(\frac{\tilde{P}_1 + \sin \tilde{L}}{\Phi(\tilde{L})} + \sin \tilde{L} \right) a_\theta - \right. \\
 &\quad \left. \tilde{P}_2 \frac{\tilde{Q}_1 \cos \tilde{L} - \tilde{Q}_2 \sin \tilde{L}}{\Phi(\tilde{L})} a_h \right] \\
 \frac{dP_2}{dt} &= B \sqrt{\frac{\tilde{a}}{\mu}} \left[a_r \sin \tilde{L} + \left(\frac{\tilde{P}_2 + \cos \tilde{L}}{\Phi(\tilde{L})} + \cos \tilde{L} \right) a_\theta + \right. \\
 &\quad \left. \tilde{P}_1 \frac{\tilde{Q}_1 \cos \tilde{L} - \tilde{Q}_2 \sin \tilde{L}}{\Phi(\tilde{L})} a_h \right] \\
 \frac{dQ_1}{dt} &= \frac{B}{2} \sqrt{\frac{\tilde{a}}{\mu}} (1 + \tilde{Q}_1^2 + \tilde{Q}_2^2) \frac{\sin \tilde{L}}{\Phi(\tilde{L})} a_h \\
 \frac{dQ_2}{dt} &= \frac{B}{2} \sqrt{\frac{\tilde{a}}{\mu}} (1 + \tilde{Q}_1^2 + \tilde{Q}_2^2) \frac{\cos \tilde{L}}{\Phi(\tilde{L})} a_h
 \end{aligned} \tag{22}$$

where L is the true longitude, $B = \sqrt{1 + \tilde{P}_1^2 + \tilde{P}_2^2}$, $\Phi(\tilde{L}) = 1 + \tilde{P}_1 \sin \tilde{L} + \tilde{P}_2 \cos \tilde{L}$, and

D. Evidence-based Robust Optimisation

This paper uses the change of Probability of Collision after and before deflection (ΔP_c) to quantify the deflection efficiency:

$$f(\mathbf{d}, \mathbf{u}) = P'_c - P_c = \Delta P_c \tag{23}$$

where decision vector $\mathbf{d} \in D$ and uncertain vector $\mathbf{u} \in U$. For NED, KI, LA missions, the decision vector consists of two elements: the epoch of launch and the time of transfer. For GT and IBS mission, the decision vector consists of three elements: the epoch of launch, the time of transfer and oversising coefficient [12]. For impulsive methods, the state and system parameters of the spacecraft before deflecting the asteroid are obtained by solving Lambert's problem. For slow-push methods, the state and system parameters of the spacecraft before deflecting the asteroid are obtained by spherical shaping method [18]. The launched performance of Delta IV Heavy-RS-68A upgrade version, which is shown in Figure 2, is considered in the robust optimisation process.

Then, the following multi-objective optimisation problem can be formed in order to maximise the Belief (Bel) in the optimal value of ΔP_c :

$$\begin{aligned}
 &\max_{\mathbf{d} \in D} Bel(-f(\mathbf{d}, \mathbf{u}) < \nu) \\
 &\min_{\mathbf{u} \in U} \nu
 \end{aligned} \tag{24}$$

The optimal design vector and thresholds that yield a $Bel = 1$ for all possible $\mathbf{u} \in U$ can be computed solving the following classic min-max problem [10]:

$$\min_{\mathbf{d} \in D} \max_{\mathbf{u} \in U} f(\mathbf{d}, \mathbf{u}) \tag{25}$$

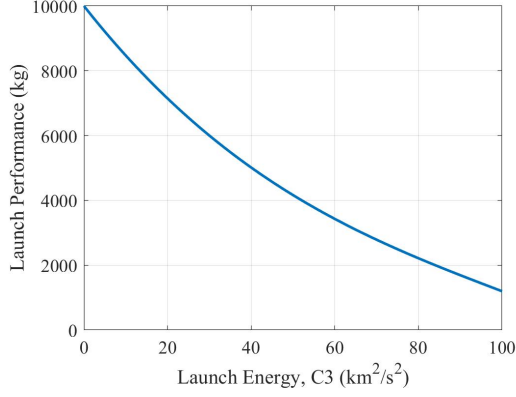


Figure 2. Launch performance of Delta IV Heavy-RS-68A upgrade version.

Because the focal elements in \mathcal{U} can be overlapping or disconnected, the calculation of $f(\mathbf{d}, \mathbf{u})$ needs to explore each focal element independently and therefore face an exponential number of optimisation problems. The exponential complexity can be avoided by collecting all focal elements, through an affine transformation [19], into a compact unit hypercube $\bar{\mathcal{U}}$ that all focal elements are adjacent and not overlapping. Finally, the Adaptive Multi-Population Inflationary Differential Evolution Algorithm (MP-AIDEA) [20] and Sequential Quadratic Programming (SQP) are used to optimise the outer-loop and inner-loop of the min-max problem. The number of agents per population used by MP-AIDEA to search for the global optimum is 10, the number of populations is 4 and total number of calls to the objective function is 60. SQP is performed by *fmincon* function in MATLAB with the tolerance of $1e^{-6}$.

III. DATASET GENERATION

This section explains how we select the asteroids to form the set of virtual impact scenarios, and how we set the classification criterion and generate the dataset for training Asteroid Impact Scenarios Identifier and Asteroid Deflection Strategies Selector.

A. Virtual impact scenarios generation

Due to the fact that no asteroid that we know of that poses a significant threat to Earth, the virtual impact scenarios should be generated for training the IDSS. The procedure of generating virtual impact scenarios mainly includes two steps: step1 is to generate virtual impactors, and step2 is to apply uncertainties on virtual impactors to form the virtual impact scenarios.

Step1 (generate virtual impactors): we assume the Earth orbit is circular, therefore, two necessary but not sufficient conditions on the semi-major axis a , eccentricity e for virtual impactors are

$$\begin{cases} a(1-e) < 1\text{AU} \\ a(1+e) > 1\text{AU} \end{cases} \quad (26)$$

Fixing the semi-major axis a , eccentricity e and inclination i with their actual value from the JPL Small-Body Database

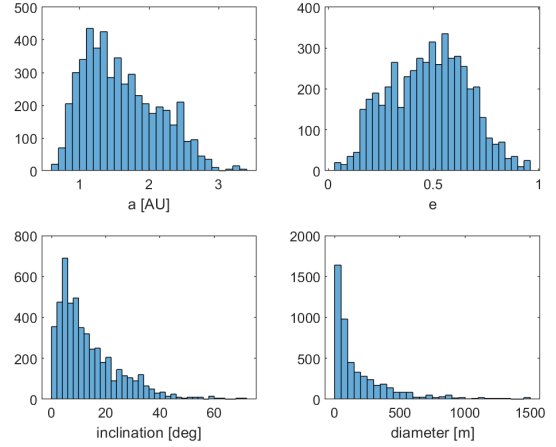


Figure 3. Distribution of Virtual Impactors.

 Table I
UNCERTAINTY INTERVALS OF $\sigma_{\mathbf{x}}$ AND σ_H

Parameters	Uncertainty Interval (Source1)	Uncertainty Interval (Source2)
σ_a [AU]	[1e-10, 1e-6]	[1e-6, 1e-1]
σ_e	[1e-8, 1e-6]	[1e-4, 1e-2]
σ_i [°]	[1e-6, 1e-4]	[1e-3, 1e-1]
σ_Ω [°]	[1e-5, 1e-3]	[1e-3, 1e-1]
σ_ω [°]	[1e-5, 1e-3]	[1e-3, 1e0]
σ_M [°]	[1e-5, 1e-3]	[1e-2, 1e0]
σ_H	[0.1, 0.5]	[0.5, 0.8]

Browser, one independent element remaining to fix is the longitude of the ascending node Ω of the asteroid's orbital plane with respect to the ecliptic plane. However, since the assumption of circular Earth orbit, the expected impact epoch t_{MOID} (time of Minimum Orbit Intersection Distance, MOID) is arbitrary and we can choose to fix $\Omega = 0$. The argument of perihelion ω and the true anomaly θ are determined by [12]

$$\begin{cases} 1\text{AU} = \frac{a(1-e^2)}{1+e\cos\omega} \\ \theta = 2\pi - \omega \end{cases} \quad (27)$$

11,619 asteroids pass the above filters and form the virtual impactors. We randomly select 5000 of them to apply the uncertainties on orbital elements \mathbf{x} and absolute visual magnitude H , which further form the virtual impact scenarios. Figure 3 shows the distribution of 5000 virtual impactors.

Step2 (apply uncertainties on virtual impactors): To get the reasonable uncertainty intervals ($[\underline{\sigma}, \bar{\sigma}]$) of $\sigma_{\mathbf{x}}$ and σ_H , we count the distribution of real $\sigma_{\mathbf{x}}$ and σ_H from the JPL Small-Body Database Browser, then the two reasonable uncertainty intervals for $\sigma_{\mathbf{x}}$ and σ_H are summarized in Table III-A.

The warning time are randomly collected from [1, 10] years and uncertainty Intervals $[\underline{\sigma}, \bar{\sigma}]$ of $\sigma_{\mathbf{x}}$ and σ_H are randomly sampled from two sources listed in Table III-A. Finally, we generated a total of 15,000 virtual impact scenarios. Among these, one third using two equally reliable sources of uncertainty interval ($bpa_{\text{Source1}} = bpa_{\text{Source2}} = 0.5$),

Table II
DESCRIPTION OF THE CLASSES IN THE IDENTIFIER

Class	Description	Decision
1	Short-term high risk or short-term high uncertainty	Deflection
2	mid-term or long-term high risk	
3	mid-term or long-term high uncertainty	More measurements required
4	long-term low risk	
5	short-term or mid-term low risk	No Deflection

one third using sources that Source1 is more reliable than Source2 ($bpa_{Source1} = 0.9, bpa_{Source2} = 0.1$), one third using sources that Source2 is more reliable than Source1 ($bpa_{Source1} = 0.1, bpa_{Source2} = 0.9$).

B. Classification Criterion

1) *Asteroid Impact Scenarios Identifier*: For each virtual impact scenario, by using the UT technique under the framework of DSt, the Belief & Plausibility curves of P_c at the expected impact epoch can be obtained. Based on the Belief & Plausibility curves of P_c , the virtual impact scenarios are classified by 5 classes. Table III-B1 shows the description and corresponding decision of each class, among these only the Class 1 and Class 2 can activate Asteroid Deflection Strategies Selector.

The classification criterion use the warning time (t_{warn}), Belief (Bel) & Plausibility (Pl) and the Degree of Uncertainty (DoU) of P_C being greater than a certain value. The warning time is divided in to 3 types: short-term ($t_{warn} < T_1$), mid-term ($T_1 < t_{warn} < T_2$) and long-term ($t_{warn} > T_2$). The Bel and DoU supporting the value of P_C greater than a threshold P_{C0} can be described as $Bel|_{P_{C0}}$ and ($DoU|_{P_{C0}} = Pl|_{P_{C0}} - Bel|_{P_{C0}}$). Table III-B1 shows the classification criterion of Asteroid Impact Scenario Identifier, while the threshold parameters are setting as $P_{C0} = 10^{-4}$, $Bel_0 = 0.6$, $\Delta = 0.3$, $T_1 = 5$ years and $T_2 = 10$ years. Figure 4 shows the unbalanced and balanced dataset of Asteroid Impact Scenarios Identifier. From the left side of Figure 4, it can be seen that Class 1 and Class 3 are underrepresented. Simulation test results show that the performance of Asteroid Impact Scenarios Identifier was negatively affected by unbalanced class distribution. Finally a new balanced dataset which contains about 600 samples per class (right side of Figure 4) was generated for training Asteroid Impact Scenarios Identifier.

2) *Asteroid Deflection Strategies Selector*: For each virtual impact scenario, we perform a robust optimisation, under mixed aleatory/epistemic uncertainties, of the deflection scenario with five different deflection strategies. The deflection efficiency (calculated by robust solution) is used to rank the deflection strategies. KI, LA, GT and IBS is applied first, if none of them provides sufficient deflection then NED is applied. The 'sufficient deflection' is defined as $\Delta P_c > 10^{-12}$. Table III-B2 shows the definition of Selector's 4 classes. Finally, the dataset used for training Asteroid Deflection Strategies Selector is shown in Figure 5.

Table III
CLASSIFICATION CRITERION OF THE IDENTIFIER

Warning time	Belief at P_{c0}	Degree of Uncertainty (DoU) at P_{c0}	Class
$t_{warn} < T_1$	$Bel _{P_{c0}} \geq Bel_0$		1
	$Bel _{P_{c0}} < Bel_0$	$DoU _{P_{c0}} \leq \Delta$	5
$T_1 < t_{warn} < T_2$	$Bel _{P_{c0}} < Bel_0$	$DoU _{P_{c0}} > \Delta$	1
			2
	$Bel _{P_{c0}} \geq Bel_0$	$DoU _{P_{c0}} \leq \Delta$	5
		$DoU _{P_{c0}} > \Delta$	3
$t_{warn} > T_2$	$Bel _{P_{c0}} \geq Bel_0$		2
	$Bel _{P_{c0}} < Bel_0$	$DoU _{P_{c0}} \leq \Delta$	4
		$DoU _{P_{c0}} > \Delta$	3

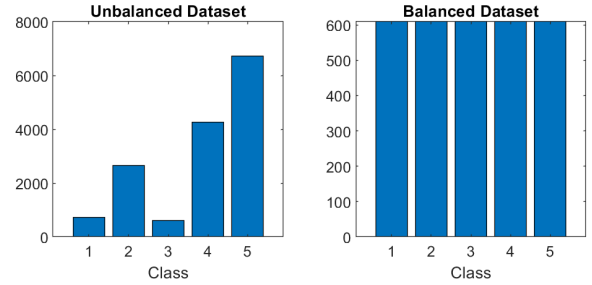


Figure 4. Unbalanced & Balanced dataset of Identifier.

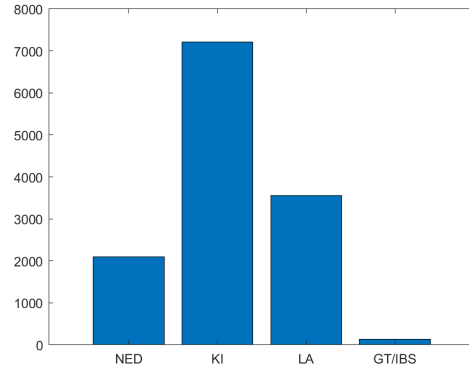


Figure 5. Dataset of Selector.

Table IV
DESCRIPTION OF THE CLASSES IN THE SELECTOR

Class	Description
NED	Nothing available but NED
KI	Except NED, KI's performance is the best
LA	Except NED, LA's performance is the best
GT/IBS	Except NED, GT or IBS's performance is the best

Table V
CLASSIFICATION RESULTS OF IDENTIFIER

Technique	Class	Accuracy	Precision	Recall	F1
RF	Overall	82.34			82.27
	1		89.51	91.43	90.46
	2		74.21	96.58	83.93
	3		79.33	80.95	80.13
	4		86.61	73.33	79.42
	5		85.71	70.59	77.42
DNN	Overall	84.1			84.12
	1		90.21	92.14	91.17
	2		75.27	93.84	83.54
	3		82.89	85.71	84.28
	4		90.7	78	83.87
	5		84.62	71.9	77.74
CNN	Overall	82.72			82.51
	1		90.26	96.17	93.12
	2		74.01	95.45	83.37
	3		78.53	82.87	80.65
	4		83.23	73.54	78.09
	5		91.43	67.02	77.34

IV. PERFORMANCE OF INTELLIGENT DECISION SUPPORT SYSTEM

This section we will discuss the performance of Asteroid Impact Scenarios Identifier and Asteroid Deflection Strategies Selector. The performance of RF, DNN, CNN are obtained by predicting the labels of samples in the validation set. The metrics employed to assess the model are: the overall accuracy, the precision by class, the recall by class, the F1-score by class, and the mean F1-score. The hyperparameters refer to the Ref. [21]. For each classifier, Asteroid Impact Scenarios Identifier and Asteroid Deflection Strategies Selector, we use 80% of the samples for training and 20% for testing.

$$F_1 = 2 \frac{\text{recall} * \text{precision}}{\text{recall} + \text{precision}} \quad (28)$$

A. Asteroid Impact Scenarios Identifier

Table IV-A shows the classification results of Asteroid Impact Scenarios Identifier. It can be seen that DNN technique performs better than RF and CNN, both in total accuracy and mean F1-score. The mean F1-score of Asteroid Impact Scenarios Identifier based on DNN is 84.12. The high recall of Class 1 and Class 2 indicate that some 'More measurements required' or 'No deflection' samples are mis-labeled as 'Deflection' (some false negative Class 3, 4, 5 tend to be classified as Class 1 or Class 2). This means Asteroid Impact Scenarios Identifier is currently rather conservative that shows the high recognition for dangerous asteroid impact scenarios.

B. Asteroid Deflection Strategies Selector

Table IV-B shows the classification results of Asteroid Deflection Strategies Selector. It can be seen that RF technique performs better than DNN and CNN, both in total accuracy and mean F1-score. The mean F1-score of Asteroid Deflection Strategies Selector based on RF is 90.27. The F1-score of KI and LA reach to 94. Due to the limited number of samples labeled with Class GT/IBS in the dataset (as shown in Figure 5), more false negative samples exist in the Class GT/IBS. However, with the consideration of longer warning

Table VI
CLASSIFICATION RESULTS OF SELECTOR

Technique	Class	Accuracy	Precision	Recall	F1
RF	Overall	93.27			90.27
	NED		93.53	84.68	88.89
	KI		91.65	96.92	94.21
	LA		96.57	92.04	94.25
	GT/IBS		100	72	83.72
DNN	Overall	91.81			88.33
	NED		88.29	88.29	88.29
	KI		92.62	93.27	92.95
	LA		92.42	91.76	92.09
	GT/IBS		90	72	80
CNN	Overall	89.08			84.61
	NED		85.91	80.18	82.95
	KI		89.71	91.69	90.69
	LA		89.6	90.01	89.81
	GT/IBS		87.5	65.63	75

Table VII
INFORMATION OF A VIRTUAL IMPACT SCENARIO

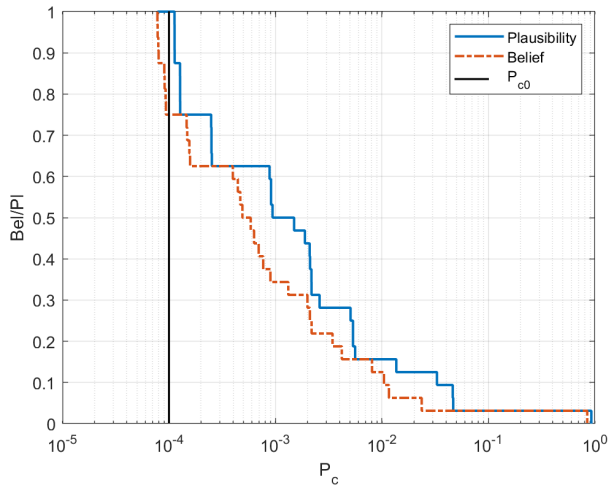
Item	Nominal	σ Interval (Source1)	σ Interval (Source2)
a [AU]	1.006	[3.013e-07, 8.467e-07]	[0.005, 0.006]
e	0.23	[3.947e-07, 6.336e-07]	[0.003, 0.004]
i [°]	1.5994	[3.716e-05, 6.285e-05]	[0.093, 0.095]
Ω [°]	0	[8.403e-05, 9.983e-04]	[0.042, 0.083]
ω [°]	101.86	[9.603e-04, 9.777e-04]	[0.687, 0.780]
M [°]	-75.35	[9.781e-04, 9.933e-04]	[0.042, 0.167]
H	22.7	[0.205, 0.467]	[0.758, 0.785]

time ($t_{warn} > 10$ years) in the future work, more and more samples labeled with Class GT/IBS will be included in the dataset, therefore the classification performance of the Class GT/IBS will be improved.

C. Example: Virtual impact scenario (asteroid 54509 YORP)

To intuitively show the performance of IDSS (consists of Asteroid Impact Scenarios Identifier and Asteroid Deflection Strategies Selector), in this section we test IDSS under a virtual impact scenario of asteroid 54509 YORP (2000 PH5). The diameter of asteroid YORP is about 97.67 m, and its corresponding virtual impact scenario's information is listed in Table IV-C with assumptions of $t_{warn} = 8$ years and $bpa_{source1} = bpa_{source2} = 0.5$. Figure 6 shows the Belief and Plausibility curves of P_c at the time of MOID. As its $Bel|_{P_{c0}} = 0.8581$ and $DoU|_{P_{c0}} = 0.1419$, this virtual impact scenario belongs to Class 2 according to the criterion in Table III-B1. The computation time of Belief and Plausibility curves is totally 47.35s. Class 2 indicates the virtual impact scenario is dangerous enough to perform the deflection. Table IV-C shows robust optimisation results of 5 different deflection strategies, and LA is suggested to be the most efficient and robust strategy. The computation time of robust optimisation for 5 deflection strategies is totally 321.72s.

The IDSS is then tested on this virtual impact scenario, simulation results show that both of the Asteroid Impact Scenarios Identifier and the Asteroid Deflection Strategy Selector can predict the classes correctly with the total computation time less than 5s.

Figure 6. Belief and Plausibility curves of P_c .Table VIII
ROBUST OPTIMISATION RESULTS FOR 5 DEFLECTION STRATEGIES

Strategy	Optimal worst cases (ΔP_c)
NED	-7.49E-05
KI	-2.46E-05
LA	-4.47E-04
GT	-1.20E-06
IBS	-6.93E-05

V. CONCLUSION

This paper proposes the Intelligent Decision Support System (IDSS) that consists of The Asteroid Impact Scenarios Identifier and Asteroid Deflection Strategies Selector. The Asteroid Impact Scenarios Identifier is designed to automatically decide if a further deflection action is necessary to respond to an asteroid impact scenario. The Asteroid Deflection Strategies Selector is designed to automatically assess the most efficient and robust deflection strategy to respond to an asteroid impact scenario. The capabilities of Random Forest, Deep Neural Networks and Convolutional Neural Networks at classifying impact scenarios and deflection strategies are shown in this paper. Simulation results suggest that the proposed system can quickly provide decisions to respond to an asteroid impact scenario.

ACKNOWLEDGMENT

The authors express their gratitude to Luis Sanchez Fernandez-Mellado for his help in implementing the Patera's method, Random Forest and Deep Neural Networks.

REFERENCES

- [1] Introduction of planetary defense. <https://www.nasa.gov/planetarydefense/faq>. Accessed Jun 6, 2022.
- [2] David SP Dearborn, Megan Bruck Syal, Brent W Barbee, Galen Gisler, Kevin Greenaugh, Kirsten M Howley, Ronald Leung, Joshua Lyzhof, Paul L Miller, Joseph A

- Nuth, et al. Options and uncertainties in planetary defense: Impulse-dependent response and the physical properties of asteroids. *Acta Astronautica*, 166:290–305, 2020.
- [3] Siegfried Eggl, Daniel Hestroffer, Juan L Cano, Javier Martín Ávila, Line Drube, Alan W Harris, Albert Falke, Ulrich Johann, Kilian Engel, Stephen R Schwartz, et al. Dealing with uncertainties in asteroid deflection demonstration missions: Neotwist. *Proceedings of the International Astronomical Union*, 10(S318):231–238, 2015.
- [4] Sung Wook Paek. *Asteroid deflection campaign design integrating epistemic uncertainty*. PhD thesis, Massachusetts Institute of Technology, 2016.
- [5] Shinsuke Abe, Tadashi Mukai, Naru Hirata, Olivier S Barnouin-Jha, Andrew F Cheng, Hirohide Demura, Robert W Gaskell, Tatsuaki Hashimoto, Kensuke Hiraoka, Takayuki Honda, et al. Mass and local topography measurements of itokawa by hayabusa. *Science*, 312(5778):1344–1347, 2006.
- [6] Glenn Shafer. *A mathematical theory of evidence*. Princeton university press, 1976.
- [7] Md Asadujjaman and Kais Zaman. Robustness-based portfolio optimization under epistemic uncertainty. *Journal of Industrial Engineering International*, 15(2):207–219, 2019.
- [8] Massimiliano Vasile and Nicolas Thiry. Nuclear cypher: An incremental approach to the deflection of asteroids. *Advances in Space Research*, 57(8):1805–1819, 2016.
- [9] Massimiliano Vasile and Camilla Colombo. Optimal impact strategies for asteroid deflection. *Journal of guidance, control, and dynamics*, 31(4):858–872, 2008.
- [10] Federico Zuiani, Massimiliano Vasile, and Alison Gibbings. Evidence-based robust design of deflection actions for near earth objects. *Celestial Mechanics and Dynamical Astronomy*, 114(1):107–136, 2012.
- [11] Edward T Lu and Stanley G Love. Gravitational tractor for towing asteroids. *Nature*, 438(7065):177–178, 2005.
- [12] Nicolas Thiry and Massimiliano Vasile. Statistical multi-criteria evaluation of non-nuclear asteroid deflection methods. *Acta Astronautica*, 140:293–307, 2017.
- [13] Steven R Chesley, Paul W Chodas, Andrea Milani, Giovanni B Valsecchi, and Donald K Yeomans. Quantifying the risk posed by potential earth impacts. *Icarus*, 159(2):423–432, 2002.
- [14] Simon J Julier, Jeffrey K Uhlmann, and Hugh F Durrant-Whyte. A new approach for filtering nonlinear systems. In *Proceedings of 1995 American Control Conference-ACC'95*, volume 3, pages 1628–1632. IEEE, 1995.
- [15] Ya-zhong Luo and Zhen Yang. A review of uncertainty propagation in orbital mechanics. *Progress in Aerospace Sciences*, 89:23–39, 2017.
- [16] Russell P Patera. General method for calculating satellite collision probability. *Journal of Guidance, Control, and Dynamics*, 24(4):716–722, 2001.
- [17] Hanspeter Schaub and John L Junkins. *Analytical me-*

chanics of space systems. Aiaa, 2003.

- [18] Daniel M Novak and Massimiliano Vasile. Improved shaping approach to the preliminary design of low-thrust trajectories. *Journal of guidance, control, and dynamics*, 34(1):128–147, 2011.
- [19] Massimiliano Vasile, Edmondo Minisci, Federico Zuiani, Eirini Komninou, and Quirien Wijnands. Fast evidence-based space system engineering. In *62nd International Astronautical Congress*, pages 1–12, 2011.
- [20] Marilena Di Carlo, Massimiliano Vasile, and Edmondo Minisci. Adaptive multi-population inflationary differential evolution. *Soft Computing*, 24(5):3861–3891, 2020.
- [21] Luis Sánchez Fernández-Mellado and Massimiliano Vasile. On the use of machine learning and evidence theory to improve collision risk management. *Acta Astronautica*, 181:694–706, 2021.